Earth and Planetary Science Letters 498 (2018) 101–115

Contents lists available at ScienceDirect

Earth and Planetary Science Letters

www.elsevier.com/locate/epsl

Paleomagnetic evidence for upper plate response to a STEP fault, SW Anatolia

Nuretdin Kaymakcı [a,*], Cor Langereis [b], Murat Özkaptan [c], A. Arda Özacar [a], Erhan Gülyüz [d], Bora Uzel [e], Hasan Sözbilir [e]

[a] Department of Geological Engineering, Middle East Technical University (METU/ODTU), Dumlupinar Bulvari 1, 06800 Ankara, Turkey
[b] Department of Earth Sciences, Utrecht University, Budapestlaan 17, 3584 CD Utrecht, the Netherlands
[c] Department of Geophysical Engineering, Karadeniz Technical University, TR-61080 Trabzon, Turkey
[d] Department of Geological Engineering, Van Yüzüncüyıl University, TR-65080 Van, Turkey
[e] Department of Geological Engineering, Dokuz Eylül University, Tınaztepe Campus, 35160-İzmir, Turkey

ARTICLE INFO

Article history:
Received 7 April 2018
Received in revised form 11 June 2018
Accepted 14 June 2018
Available online 4 July 2018
Editor: A. Yin

Keywords:
STEP fault
Pliny-Strabo Trench
SW Anatolia
Fethiye Burdur Fault Zone
paleomagnetism
vertical axis rotation

ABSTRACT

Pliny-Strabo Trench is a Subduction Transform-Edge Propagator (STEP) Fault developed on the northern edge of the subducted African Oceanic Lithosphere. It connects the Aegean and Cyprian trenches in the Eastern Mediterranean convergent system. Although, deep geometry of the STEP fault and associated slab tear in mantle are imaged, its shallow vertical and lateral continuation in the crust and impact on the over-riding plate are still unknown. Thus, we have studied SW Anatolia, the candidate site where this structure could propagate laterally and vertically, for its vertical axis rotations using paleomagnetic tools. In this study, more than 2000 paleomagnetic samples were collected and analysed from 86 different sites which were later classified into 11 separate geographic domains displaying similar tectonic characteristics. Moreover, available paleomagnetic data in the literature were parametrically resampled, analysed and combined with our data. In the region, there is a positive correlation between rotation amounts and sample ages supporting continuous deformation throughout the Neogene period. The spatial variations of results indicated that the study area can be divided into three main domains based on vertical axis rotations. From the south to the north these domains include SW Anatolian domain with ~20° counter-clockwise rotation, Burdur–Dinar–Ulubey domain with ~4° counter-clockwise rotation and northern areas characterized by clockwise rotations. The identified domains of counter-clockwise rotation are separated by a well-defined NW-SE striking Acıpayam Transfer Zone and there is no differential rotation in agreement with the presence of NE-SW striking shear zone in the region. Therefore, we concluded that the Pliny-Strabo STEP Fault have not propagated into the over-riding plate as a shear zone. This implies that there is no evidence to support the presence of alleged Fethiye–Burdur Fault Zone as suggested, and its existence is dubious.

1. Introduction

Much of the convergent strain due to African-Eurasian convergence in Eastern Mediterranean region is taken up along the Hellenic-Cyprian subduction system which extends from Adriatic Sea in the west and Levant in the east (Fig. 1) along which the oceanic crust of northern edge of African Plate subducts northwards beneath the southern edge of Eurasia. Recent studies, mainly based on mantle tomography, demonstrated that the edge of the subducted African lithosphere is detached and, in places, torn apart at high angle to the trench (Wortel and Spakman, 2000; Faccenna et al., 2006; van Hinsbergen et al., 2010c; Biryol et al., 2011; Salaün et al., 2012) such structures are named as Subduction Transform-Edge Propagator (STEP) fault (terminology after Govers and Wortel, 2005). One of the most peculiar of these STEP Faults developed in the SE Aegean region surface manifestation of which is the Pliny-Strabo Trench (van Hinsbergen et al., 2010c; Özbakir et al., 2013). To the east of the Karasu–Latakia Fault, the Afro-Arabian slab completely detached along the Bitlis-Zagros Suture Zone during the Early to Middle Miocene following the collision between Arabian and Eurasian plates (Faccenna et al., 2006; Kaymakci et al., 2010; Biryol et al., 2011). Similarly, the tomographic images (Biryol et al., 2011) indicate that the subduction angle of the Cyprian Slab is shallower below central Anatolia and

* Corresponding author.
E-mail address: kaymakci@metu.edu.tr (N. Kaymakcı).

https://doi.org/10.1016/j.epsl.2018.06.022
0012-821X/

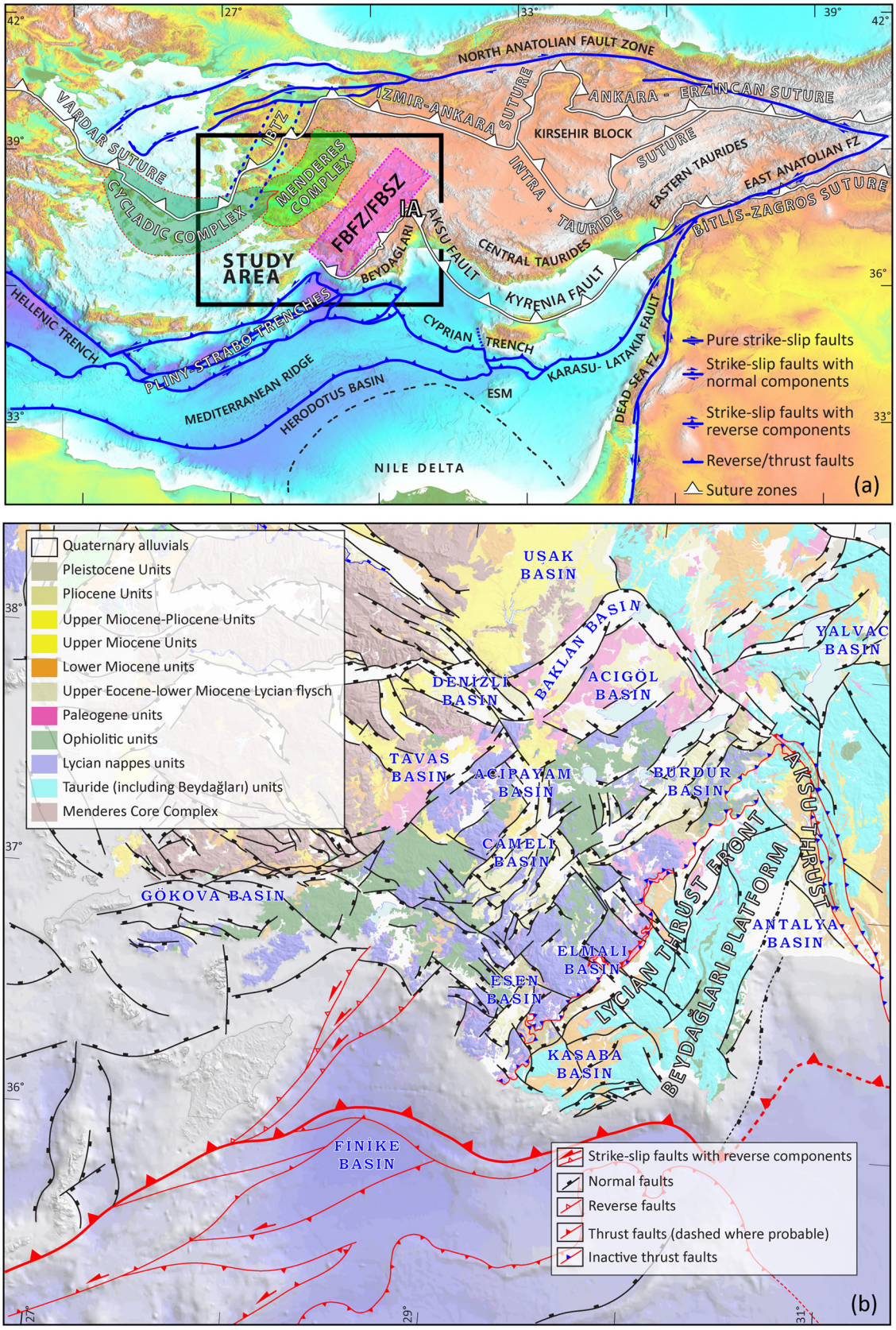

Fig. 1. (a) Simplified tectonic scheme of the Eastern Mediterranean Region. ESM: Eratosthenes Sea Mount. FBFZ/FBSZ: location of the alleged Fethiye Burdur Fault/Shear Zone (Hall et al., 2014). IA: Isparta Angle. IBTZ: İzmir–Balıkesir Transfer Zone (Uzel et al., 2013, 2015). (b) Simplified geological map of the study area (Özkaptan et al., 2018). (For interpretation of the colours in the figure(s), the reader is referred to the web version of this article.)

towards the north, it becomes steeper. The tear to the north of Pliny-Strabo STEP Fault, resulted in a mantle window below the western Anatolia. The eastern edge of this window corresponds to the western margin of the Isparta Angle on map view and the western edge corresponds to the İzmir–Balıkesir Transfer Zone (Uzel et al., 2013, 2015). By nature the surface expressions of STEP faults may resemble, in many ways, to strike-slip fault zones and could bear similar deformation styles and mechanism. However, the STEP faults are developed at a point and propagates asymmetrically only in a direction opposite to direction of the subduction. This results in gradual increase in the vertical axis rotations, migration of locus of extension and younging of the depositional environments over the overriding plate as the depocenter migrated from the point of tear towards the trench (Govers and Wortel, 2005).

It is suggested that the Pliny-Strabo Trench propagated onland in SW Anatolia and developed Fethiye Burdur Fault Zone (FBFZ). It was first proposed by Dumont et al. (1979), and later Barka and Reilinger (1997) suggested that it might be a sinistral strike-slip fault zone linked to the Pliny-Strabo Trench. After these studies a very large literature have been accumulated about the fault zone, most of which took these claim as granted, although no convincing evidence was provided for the presence, geometry and kinematics of such a fault zone, and based on their interpretations in favour of alleged sinistral strike-slip nature of the FBFZ. Recently, Hall et al. (2014) and Elitez et al. (2016) argued that it is not a single or a narrow fault zone but a wide sinistral transtensional shear zone, as wide as ∼80 km, which makes its detection and recognition, in the field, difficult. They also argued that the Fethiye–Burdur Shear Zone is the northwards continuation of the Pliny-Strabo Trench into the SW Anatolian continental crust along the western margin of the Isparta Angle. They further claimed that the STEP fault zone encompasses the area between Beydağları in the east, Menderes Massif in the west, northern tip of Isparta Angle in the north and the Aegean Trench in the south (Fig. 1).

Kaymakci et al. (2017) and Alçiçek (2015) criticized and claimed that no convincing evidence has been provided for the existence and strike-slip nature of the fault zone, no matter if it is a discrete fault or a shear zone. Interestingly, kinematic evidence provided by the works in favour of FBFZ, such as fault slip data, earthquake moment tensor solutions, and GPS velocities (Barka and Reilinger, 1997; Elitez and Yaltırak, 2016; Elitez et al., 2016) indicate dominantly extensional character of the deformation in the region and there is no significant differential motion on either side of the alleged Fethiye Burdur Shear Zone that indicate strike-slip faulting. Hall et al. (2014) also argued that, to identify the true nature of the zone, one must compare the style of deformation of the shear zone and the blocks bounding it. They used analog models developed by Philippon et al. (2015) as the example of a transtensional shear zone, which could develop when the extension direction and pre-existing weakness zones are oblique to each other but they failed to indicate the existence and cause of such an inherited zone of weakness. They used possible development mechanism as the evidence of existence of the structure.

In this context, this study aimed at investigating the interaction between the Pliny-Strabo STEP Fault and over-riding plate in the SW Anatolia using paleomagnetic tools. The obtained data will be used to test the existence and kinematics of the Fethiye–Burdur Fault/Shear zone in terms of scenarios related to slab detachment (Barka and Reilinger, 1997) and STEP fault development.

2. Geological setting

This study is conducted on the Neogene basins in the SW Anatolia comprising the area from the Aegean and Mediterranean seas, southern part of the Menderes Core-Complex, and western flank of the Isparta Angle (Figs. 1 and 2). Late Oligocene and onwards, a number of isolated continental basins have been developed during the development of the Menderes Core-Complex and emplacement of Lycian Nappes over the Beydağları Platform. The oldest of these basins include Baklan-Acıgöl-Denizli-Tavas basin complex, which developed during the Oligocene as a molasses basin related to emplacement of the Lycian Nappes (Sözbilir, 2005) and it was compartmentalized during the latest Miocene into a number of isolated fluvio-lacustrine basins, such as Didim, Milas-Ören, Muğla-Yatağan, Baklan, Denizli, Ulubey and Acıgöl basins (Fig. 2). The youngest common lithology in all of these basins is Pliocene lacustrine marls and limestones. Elmalı-Korkuteli Domain and the *so-called* Kasaba Syncline developed during the Early to Middle Miocene as a foreland basin in response to southeastwards emplacements of the Lycian Nappes over the Beydağları Platform emplacement of which continued up to the end of Serravallian. Çameli, Burdur and Eşen basins were developed during the late Miocene-Pliocene as continental fluvio-lacustrine basins in response to extensional deformation following the emplacement of the Lycian Nappes (Alçiçek, 2007; Alçiçek et al., 2013; Hayward, 1984).

3. Data and methodology

3.1. Paleomagnetic sampling

Except the Kale-Tavas Domain where Oligocene units were also included, paleomagnetic studies were conducted mainly on the Early Miocene to Pliocene units in 11 domains. In total, 2300 oriented cylindrical paleomagnetic samples were collected from 86 localities, Except few, most of these sites comprise nearly complete stratigraphy from the Middle Miocene to Pliocene (Alçiçek, 2007; Alçiçek et al., 2005, 2013, 2017; Hayward, 1984; Kaymakci, 2006; Özkaptan et al., 2018; Sözbilir, 2005; Konak and Şenel, 2002) (Table 1). All of the sampled localities, except UL3, where basalt flow was sampled, were obtained from sedimentary rocks comprising fluvio-lacustrine sandy mudstones, mudstones, marl and limestones (Table 1). At each site, typical paleomagnetic cylindrical cores (25 mm Ø) were drilled within a range of several meters using handheld water-cooled diamond-coated drill bits, portable petrol-powered motor drill or an electric drill with generator, depending on the rock type. From each site, at a minimum number of 25 samples were obtained after removing the weathered surface to reach fresh outcrops. Sampling was performed on relatively undisturbed sections away from large faults. The sample orientations as well as the bedding attitudes were always measured with a magnetic compass and corrected for the local magnetic declination (5°E) for the entire sampling period according to the IGRF model (Chulliat and Maus, 2014).

3.2. Rock magnetic analyses

Prior to demagnetization process, we aimed at least one thermomagnetic measurement for each site and rock type to determine rock magnetic characteristic and identify dominant magnetic carrier(s) of the NRM of the studied rock samples under different temperatures following the procedure describe in Huang et al. (2013). Thermomagnetic runs were performed in air using a modified horizontal translation type Curie balance with a sensitivity of $\sim 5 \times 10^{-9}$ Am^2 (Mullender et al., 1993). Approximately 30–90 mg powdered rock sample (depending on the magnetic intensity of the rock) was put into a quartz-glass sample holder and were held in place by quartz wool. Temperatures were increased in a number of heating and cooling cycles up to a maximum of 700 °C. Heating and cooling rates were 10 °C/min.

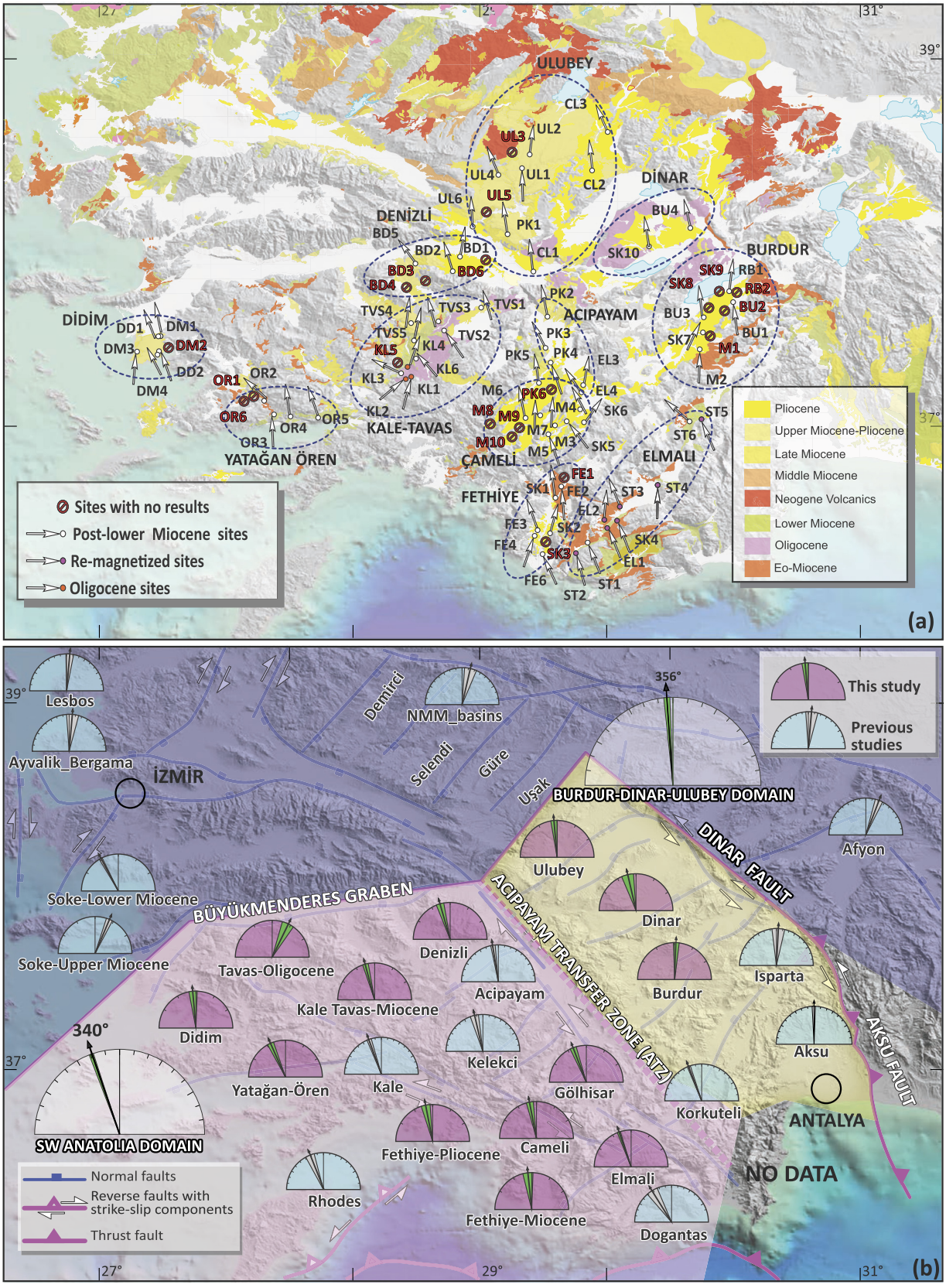

Fig. 2. (a) Paleomagnetic sample locations and declinations obtained from each sampling site. (b) Mean declinations for each domain obtained in this study and compiled from the literature. See Table 1 for their sources and details.

Table 1
Oligocene to Pliocene time interval site mean paleomagnetic results from 86 sites in the SW Anatolia. Lat: latitude of the sites; Long: longitude of the site; Nm: number of demagnetized specimens/mean ChRM direction per site under AF/TH, N_{45}: number of specimens/mean direction included in the calculation for the mean ChRM direction after applying the 45° fixed cut-off, Dec/I: declination / inclination, ΔDx / (ΔIx): errors in declination / (inclination) determined from the A95 of the poles, *k*: estimate of the precision parameter determined from the ChRM directions, a95: cone of confidence determined from the mean ChRM directions for in situ and tilt corrected data, *K*: precision parameter determined from the mean virtual geomagnetic pole directions (VGPs), λ: paleolatitude, A95: cone of confidence determined from the mean VGP direction, $A95_{min}$ / ($A95_{max}$): minimum / (maximum) value of the A95 for the given dataset based on Deenen et al. (2011). Please see Supplements for the details of each site.

Region	Site	Age	Lat. (N)	Long. (E)	Nc	ChRM directions (in situ)							ChRM directions (tilt corrected)										
						Nm/N_{45}	Dec	ΔDx	Inc	ΔIx	*k*	a95	Dec	ΔDx	Inc	ΔIx	*k*	a95	*K*	λ	$A95_{min}$	A95	$A95_{max}$
Gölhisar	Mean (N)				26	26/14	358.9	9.1	47	9.6	31.4	7.2	1.7	8.7	57.1	6.5	53.4	5.5	34.2	37.7	4.2	6.9	15.6
	Mean (R)	*Plio.*			51	51/41	156.5	6.1	−45.5	6.8	13.9	6.2	153.8	4.2	−39.4	5.4	26.9	4.4	33.8	−22.3	2.7	3.9	7.9
	Mean (N+R)		37.352	29.426	77	77/57	343.2	5.2	47	5.5	16.9	4.8	339	4.8	44.2	5.5	20.3	4.3	19.8	25.9	2.4	4.3	6.4
Burdur	Mean (N)				142	38/38	351.4	4.6	55.2	3.7	55.2	3.2	2.8	4.9	53.5	4.2	45.6	3.5	33.9	34.1	2.8	4	8.3
	Mean (R)	*Plio.*			20	20/20	173.8	4.7	−45.1	5.2	48.4	4.7	178.6	9.7	−57.3	7.2	25.6	6.6	19.3	−37.9	3.6	7.6	12.4
	Mean (N+R)		37.602	30.223	162	58/58	352.4	3.5	51.7	3.2	44.9	2.8	1.5	4.5	54.8	3.7	35.8	3.2	26.4	35.3	2.4	3.7	6.4
Çameli	Mean (R)	*U. Mi-Plio.*			157	71/67	168.8	5.8	−48.8	5.8	14.3	4.7	169.5	5.8	−49.7	5.6	14.9	4.6	12.8	−30.6	2.2	5	5.7
	Mean (N)		37.059	29.322	224	71/67	348.5	5.8	49.6	5.6	15.9	4.5	349.3	5.8	50.5	5.5	16.7	4.4	13.2	31.3	2.2	5	5.8
Denizli	Mean (N)	*L.Mio.*			104	30/30	4	4.5	51.9	4.1	74.8	3.1	344.9	8.5	61.5	5.3	40.7	4.2	18.7	42.7	3.1	4.2	9.6
	Mean (N+R)		37.823	28.804	127	45/45	352	5.7	49.1	5.6	29.4	4	344.3	6.1	58.6	4.3	42.4	3.3	21.3	39.3	2.6	4.7	7.5
Dinar	Mean (N)	*Plio.*	37.999	29.992	36	26/26	349.8	6.8	29.6	10.7	11.2	8.9	349.5	9.3	33.1	13.7	6.9	11.6	11.3	18.1	3.3	8.8	10.5
Didim	Mean (N)				38	40/17	348.4	5.7	53.8	4.8	74.1	4.2	357.8	8.8	60.7	5.7	56.1	4.8	30.3	41.7	3.9	6.6	13.8
	Mean (R)	*Plio.*			96	33/33	173.8	8	−47.2	8.4	18	6.1	174	8.2	−48.1	8.4	17.1	6.2	13	−29.2	3	7.2	9.1
	Mean (N+R)		37.427	27.335	134	50/50	352.1	5.6	49.5	5.5	23.5	4.2	355.1	6.4	52.5	5.6	20.2	4.6	15.1	33.1	2.5	5.4	7
Elmalı	Mean (N+R)	*L.-M. Mio.*	36.631	29.767	193	43/41	354.6	2.5	53.8	2.1	50.6	1.6	340.6	2.3	25.7	3.8	24.2	2.4	27	13.3	1.6	2.2	3.4
Fethiye	*Mean (N)*				37	26/26	0.6	5.7	54.2	4.7	57.9	3.8	20.5	6.4	58.6	4.5	46.5	4.2	33.8	39.4	3.3	5	10.5
	Mean ®	*Plio.*			34	11-Nov	168.7	11.4	−53.8	9.6	28.5	8.7	159	9.9	−50.7	9.3	26.6	9	30.1	−31.5	4.6	8.8	18.5
	Mean (N+R)				71	37/37	350.5	8.3	47.7	8.6	15.6	6.9	349.2	6.7	41	8.3	15.4	6.9	19.3	23.5	3.1	6.1	9.6
	Mean (N+R)	*M.Mio.*	36.548	29.362	39	19/19	353.1	10.8	42.4	13	14.1	9.5	353.9	7.8	34.9	11.2	15.9	8.7	21.5	19.2	3.7	7.4	12.8
Ören-Yatağan	Mean (N)	*L.-M. Mio.*			60	20/18	1.1	7.8	50.5	7.4	30	6.4	350	9	42.5	10.7	23.5	7.3	19	24.6	3.8	8.1	13.3
	Mean (R)				58	41/34	149.4	4.5	−42.4	5.3	40.4	3.9	150.7	5.3	−42.2	6.4	29.8	4.6	27	−24.4	2.9	4.8	8.9
	Mean (N+R)		37.219	28.004	118	60/52	337.9	5	46.4	5.4	26.1	4	336.1	4.7	42.8	5.6	27.2	3.9	22.5	24.9	2.5	4.3	6.9
Kale-Tavas	Mean (N)	*L.-Up. Mio.*			86	82/62	332.8	5.8	45	6.5	14.9	4.9	332	7	54.8	5.7	18.3	4.4	11.3	35.4	2.3	5.7	6.2
	Mean (R)	*Up. Mio.*			61	40/39	168.2	6.1	−44.6	7	19.2	5.3	158.7	6.6	−35.8	9.2	14.1	6.4	15.2	−19.8	2.8	6.2	8.3
	Mean (N+R)	*L.-Up. Mio.*			147	102/74	351.2	4.1	46.7	4.4	23.1	3.5	345.4	4.6	42.6	5.5	16	4.3	16.9	24.7	2.2	4.2	5.5
	Mean (N+R)	*Oli-L.Mio.*	37.417	28.698	48	45/45	349.7	6.3	49.2	6.3	19.1	5	25.7	9.7	43.4	11.3	14.9	8.5	14.1	25.3	3.6	8.8	12
Ulubey	Mean (N)				109	78/41	0.5	6.1	45.6	6.7	19.3	5.2	357.5	6	51.8	5.5	24.7	4.6	20.2	32.5	2.7	5.1	7.9
	Mean (R)	*Plio.*			61	41/18	169.7	9.9	−43.6	11.5	15.7	9	167.2	9.3	−40.9	11.6	15.7	9	17.3	−23.4	3.8	8.6	13.3
	Mean (N+R)		38.242	29.237	170	119/58	358.1	5	44.9	5.6	18.8	4.4	354.9	5	48.6	5	20.1	4.2	19.4	29.5	2.4	4.4	6.4
REGIONAL DOMAINS																							
Burdur–Dinar–Ulubey Domain						289/281							356	2.3	49.5	2.3	18	2	18	30.3	1.2	2	2.3
SW Anatolia Domain						653/594							340.6	1.7	42.3	2	15.2	1.5	15.4	24.5	0.9	1.5	1.5

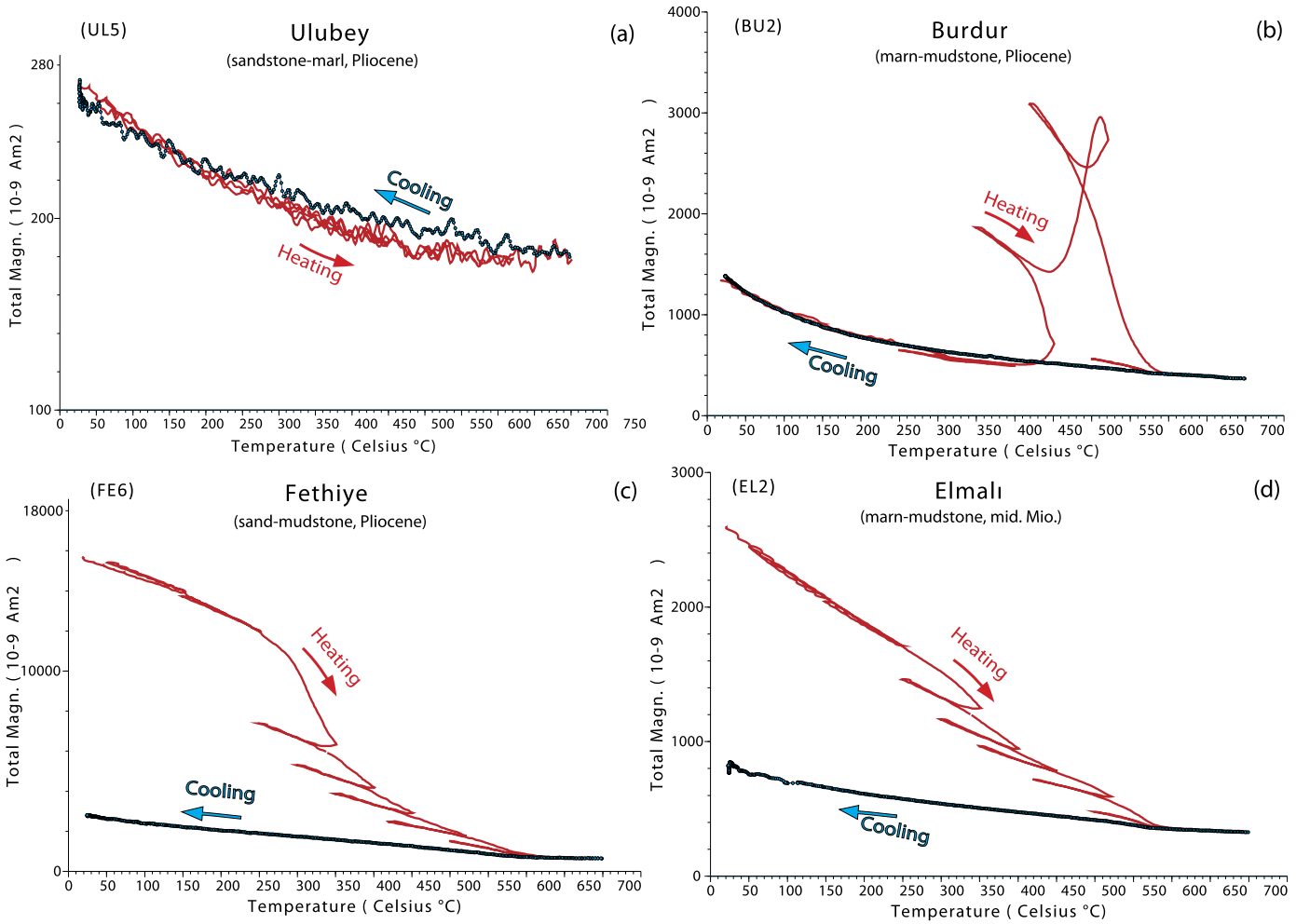

Fig. 3. Magnetic carriers identified by their characteristic thermomagnetic curves generated with the stepwise heating protocol (Mullender et al., 1993) for representative samples. Red (blue) curves demonstrate the heating (cooling) cycles. A noisy appearance is indicative of a weak magnetic signal. See the text for the explanation of the thermomagnetic behaviour.

3.3. NRM demagnetization

The oriented rock samples were cut into the standard 2.2 cm long cylindrical specimens using dual blade rock saw (ASC Scientific) with diamond-coated, water-cooled and held by a solid aluminium holder on all aluminium chassis. In most case, a single core provides two or more specimens (referred to as A and B specimens, for the deeper and shallower part of the sample respectively) which could be used for both thermal (TH) and alternating field (AF) demagnetization processes. More than 2000 samples were subjected to progressive stepwise demagnetization using thermal or/both alternating field steps. In most case, prior to AF demagnetization the specimens were heated to 150 °C and measured to remove possible viscous or present-day magnetic field effects caused by weathering, and to reduce the coercivity of the secondary overprint in the natural remnant magnetization (NRM) (Gong et al., 2008). The thermal demagnetization process was fulfilled in a magnetically shielded oven (ASC, model TD48-SC, residual field <10 nT). Each specimen was progressively demagnetized and measured by successive temperature step with increments of 20–50 °C, starting from room temperature (20 °C) and up to a maximum of 580 °C until complete demagnetization of the natural remnant magnetizations (for some samples up to a maximum of 645 °C). The alternating field ranging 0–100 mT with increment of 3–20 mT was applied for AF demagnetization process. The natural remnant magnetizations after each step was measured on a 2G Enterprises horizontal DC SQUID cryogenic magnetometer (noise level 3×10^{-12} Am^2). The AF demagnetization was performed on an in-house developed robotized and full automated sample handler attached to a horizontal pass-through 2G Enterprises DC SQUID cryogenic magnetometer (noise level 1–2 $\times$ 10^{-12} Am^2) hosted in the magnetically shielded room (Mullender et al., 2016).

4. Results

4.1. Rock magnetic properties

For each of 86 sites, at least one thermomagnetic experiment (Curie-Balance) was carried out before demagnetization processes for each lithology of site. Four representative thermomagnetic behaviour curves obtained from Curie Balance measurements are illustrated in Fig. 3. In general, the sites from different lithologies and ages show that majority of the demagnetized samples have various magnetic carriers but few sites have little or just adequate amount of ferromagnetic minerals that preserved primary magnetization (Fig. 3a). The site BU2 in the Burdur Basin illustrates an induced peak at 475–500 °C that is typical characteristics of pyrite transformation to magnetite (Fig. 3b). Some samples have reversible smooth decrease in a magnetization between 100–400 °C, continue with a sharp decline in intensity between 350–500 °C, which is characteristic for low Ti-Magnetite transforming into hematite at 350 °C and then to magnetite at 580 °C

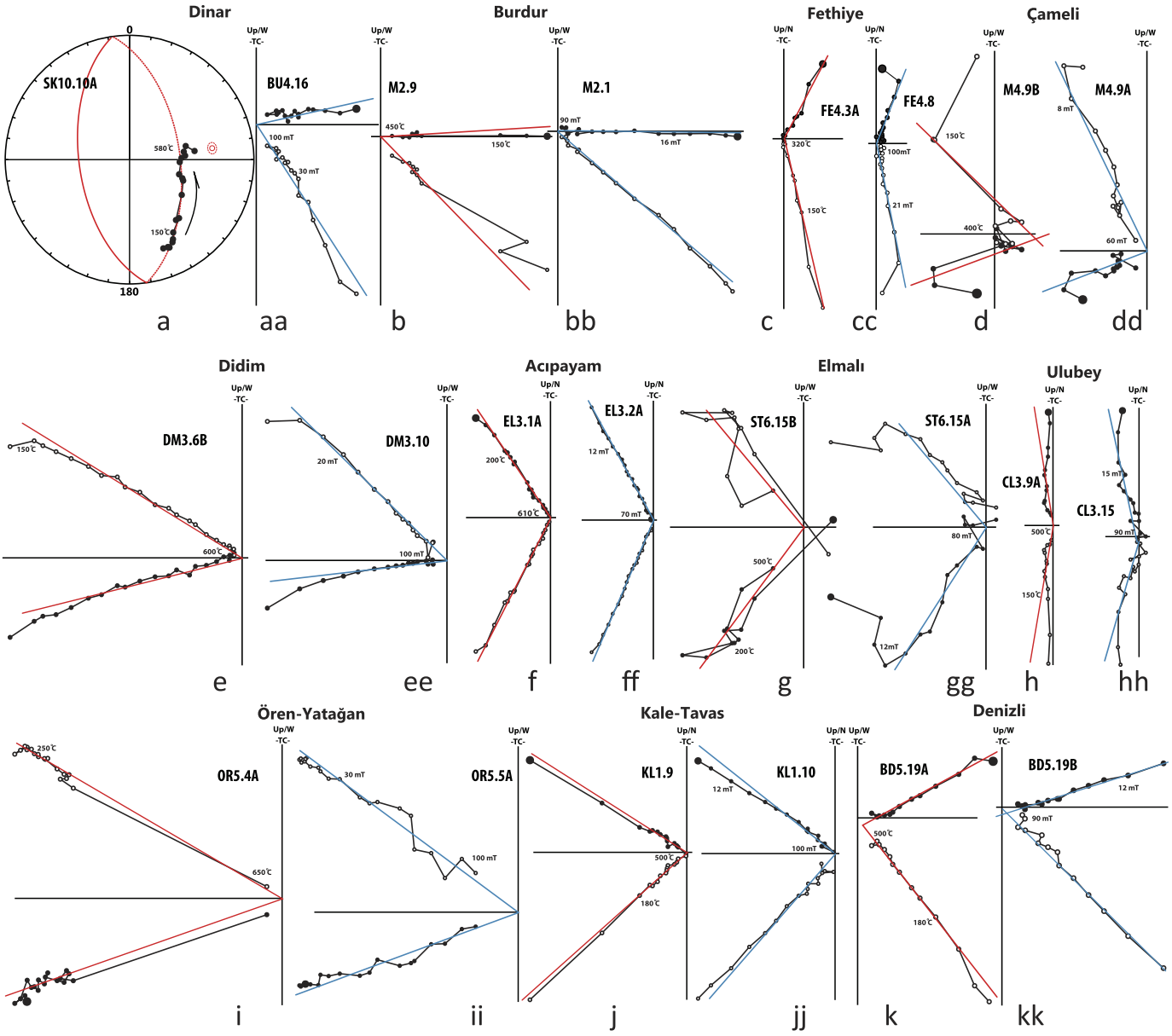

Fig. 4. Results of orthogonal vector diagrams of the representative samples demagnetized using thermal (red lines) and alternating field (blue lines). Closed (open) circles indicate the projection on the horizontal (vertical) plane. All diagrams converted to their initial bedding positions (TC). Majority, both thermal (steps in °C) and alternating field (steps n miliTesla, mT) demagnetization diagrams are shown for two specimens from the same site to compare their characteristics. (a) Great circle plot technique (McFadden and McElhinny, 1988) used to obtain the results.

(Fig. 3c). Magnetite dominant matrix shows smooth decline in intensity between 20–580 °C and is used for the paleomagnetic interpretations (Fig. 3d). Based on Curie Balance results the samples with high intensities (hematite and magnetite) were used for TH-demagnetization procedure whereas the low intensity ones were used for AF-demagnetization procedure.

4.2. ChRM directions

The ChRM (in situ/tilt corrected) and VGP directions obtained from the 86 individual sites in 11 domains, as well as the available previous published data (10 domains) are given in Tables 1 and 2 and Fig. 2. We use orthogonal vector diagrams to analyze demagnetization results (steps) of the NRM. Both AF and TH demagnetization representative results for each domain are illustrated in Fig. 4. In orthogonal diagrams, the ChRM directions were determined using principal component analysis (Kirschvink, 1980) by taking approximately five to seven or more successive points from TH or AF demagnetization steps. Few of the samples contain at least two overlapping coercivity or temperature components, were analyzed using the great circle approach (McFadden and McElhinny, 1988) (Fig. 4a). Since the results of ChRM distributions are affected by the certain amount of secular variation of the Earth's magnetic field (Deenen et al., 2011), site means (K) as well as virtual geomagnetic poles (VGP) (Fig. 5) and their means (A95, the 95% cone of confidence of the VGPs) were computed using Fisher statistics (Fisher, 1953). A fixed cut-off (45°) was applied to remove outliers as proposed by Deenen et al. (2011). VGPs per sites and the corresponding errors in declination (ΔDx) and error in inclination (ΔIx) determined individually according to Butler (1992).

The site and domain based ChRM directions are displayed on lower hemisphere, equal area projection method (Fig. 5). All demagnetization diagrams and statistical outputs were analyzed using the on-line portal Paleomagnetism.org (Koymans et al., 2016).

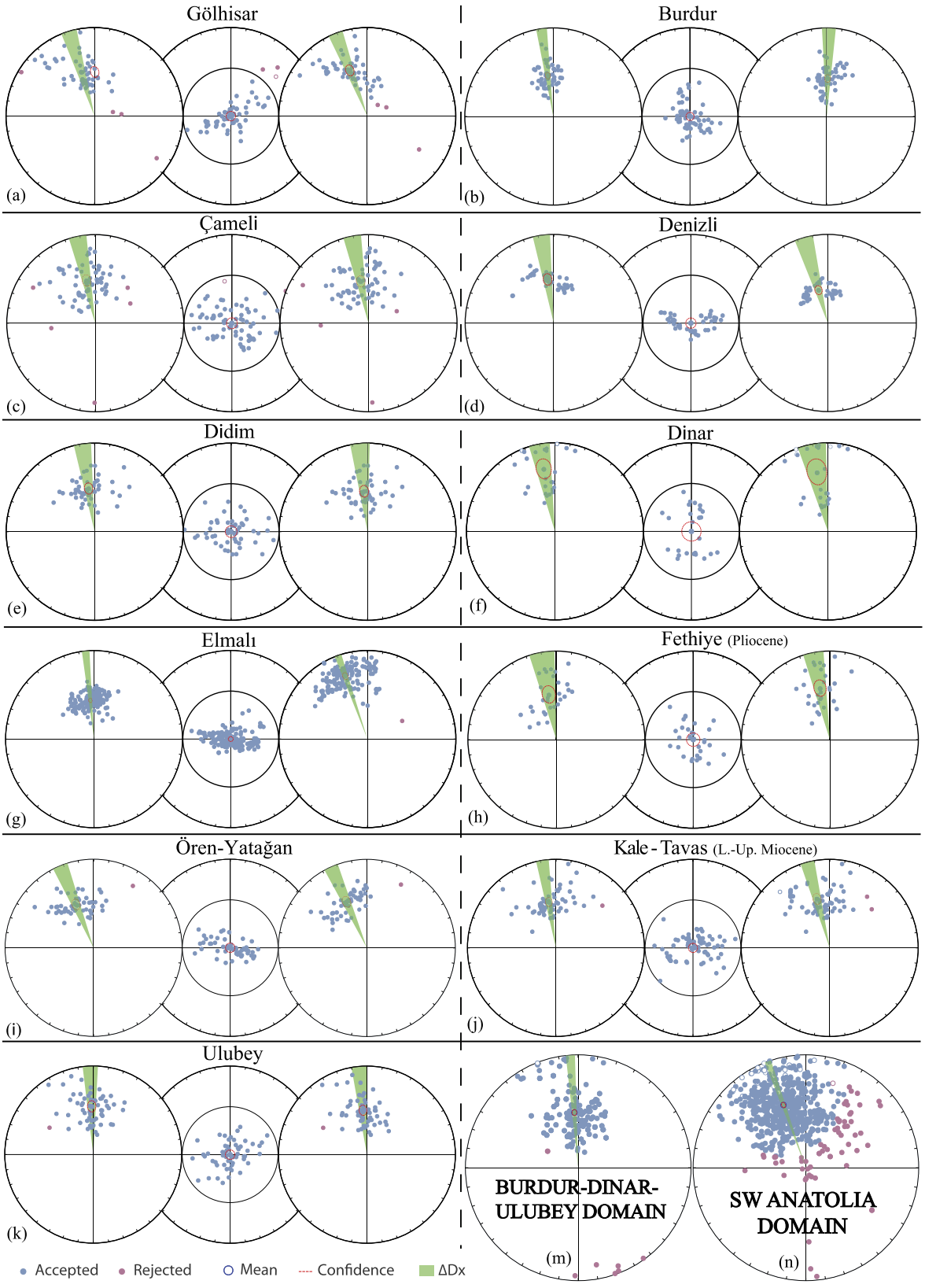

Fig. 5. Equal area projections of the ChRM and VGP directions (tilt corrected, right/in-situ, left) and their means with associated error ellipses (ΔDx, ΔIx) according to Deenen et al. (2011) of all 11 localities (Table 1). Open (solid) symbols denote projection on upper (lower) hemisphere. Large symbols indicate respectively the mean directions and their cone of confidence (a95). Magenta (small) circles indicate the individual directions rejected by 45° cut-off angle. All directions were converted to normal polarity (see also Table 1).

Table 2
Table showing all compilation of Neogene paleomagnetic results from the Southwestern Anatolia. See Table 1 for explanations.

Site	Age	Lithology	Lat.	Long.	ChRM directions (tilt corrected)									
					Dec	ΔDx	Inc	ΔIx	*k*	a95	*K*	$A95_{min}$	A95	$A95_{max}$
[1]Acıpayam	Pliocene	Shale/marl	37.4	29.4	349.4	3.3	46.3	3.6	50.4	3.0	51.6	2.6	2.9	7.3
[1]Kale	Olig-E.Mio	Limest/clayst	37.5	28.7	340	3.3	36.2	4.6	–	–	42.3	3.6	3.1	6.6
[1]Kelekci	Pliocene	Shale/marl	37.2	29.4	338.3	5.5	51.9	5.0	27.0	4.4	24.0	2.7	4.6	7.9
[1]NMM_Basins	M-L-Mio.	Volcanic.	28.7	38.8	013.4	9.2	52.7	8.0	–	–	10.2	3.9	7.7	9.1
[1]Ayvalık-Berg.	E-Mio.	Volcanic.	27.1	39.2	005.5	9.6	49.6	14.3	–	–	14.3	8.3	4.6	11.3
[1]Lesbos	E. Mio.	Volcanic.	26.4	39.2	006.3	6.2	47.9	6.3	–	–	13.0	5.4	3.4	6.0
[2]Korkuteli	E-M-Mio.	Shale/marl	29.9	36.5	340.3	2.2	31.2	3.3	12.2	2.6	18.5	1.3	2.1	2.5
[2]Doğantaş	E-M-Mio.	Shale/marl	30.1	37.1	331.4	8.6	47.9	8.9	13.7	6.9	11.6	2.9	7.6	8.9
[3]Afyon	L. Mio-Plio.	Volcanic.	30.5	38.6	020.9	6.0	45.8	6.6	14.2	5.1	13.1	2.4	5.4	6.4
[4]Rhodes	Plio-Quat.	Shale/marl	28.1	36.3	338.0	1.6	44.0	1.8	27.8	1.5	27.8	1.1	1.4	2.0
[5]Isparta	Plio.	Volcanic.	30.5	37.7	003.6	3.8	58.5	2.6	54.6	2.3	33.4	2.2	2.9	5.5
[6]Aksu	Pliocene	Shale/marl	37.3	30.9	359.6	2.5	46.1	2.6	19.5	2.2	18.3	1.3	2.2	2.6
[7]Söke	M. L. Mio.	Shale/marl	37.7	27.4	23.1	5.0	51.7	5.6	32.1	2.5	23.0	2.5	4.3	6.9

E. Early, L. Late, Mio. Miocene, Olig. Oligocene, Plio. Pliocene, Quat. Quaternary: 1. van Hinsbergen et al. (2010a), 2. van Hinsbergen et al. (2010b), 3. Gürsoy et al. (2003), 4. van Hinsbergen et al. (2007), 5. Tatar et al. (2002), 6. Koç et al. (2016). 7. Uzel et al. (2017).

Following the site mean statistical results, the accepted sites were grouped and averaged into 11 domains based on their geological characteristic and their results are listed in Table 1. The reversely polarized specimens/sites were converted to all normal polarities for statistical consistency and analyzed with the normal polarity results (Fig. 5). The results of this study as well as the previously published data were parametrically re-calculated and attributed to appropriate domains (Fig. 2 and Tables 1 and 2).

4.3. Results of each domain

Didim Domain is located at the southern flank of the Büyük Menderes Graben and lies approximately 200 m above sea level. The sampled horizons comprise upper Miocene to Pliocene sequence characterized mainly by pinkish lacustrine limestones intercalated with red mudstones. These deposits are almost undeformed but slightly tilted southwards possibly due to uplift of the shoulders of the Büyük Menderes Graben. Sampling was performed in 6 sites, which are distributed uniformly throughout the basin (Fig. 2a). Five of these sites produced reliable results. Individual sites indicate both slight clockwise and counter-clockwise rotations. Combined analysis of the domain indicate 355 ± 6°/52.5 ± 6° declination and inclination values. This implies slight (∼5°) counter-clockwise rotation (Table 1).

Ören-Yatağan Domain is located at the south-westernmost part of the study area and comprises one of the most complete Early to Middle Miocene sequence in the region. From the domain, 9 sites were sampled and four of these sites produced very reliable results. Three sites produced results with high error margin and three sites were uninterpretable due to erratic nature of the results. Almost all of the individual sites produced counter-clockwise rotations in various and combined results of the reliable sites of the domain indicate 336 ± 5°N/43 ± 6° declination and inclination values, which indicates approximately 24° counter-clockwise rotation of the domain (Figs. 2, 4, and 5).

Kale-Tavas Domain comprises two different data sets. The older data set includes Oligocene to lower Miocene sequences and the younger sequence includes upper Miocene to Pliocene rocks. The Oligocene sites include three sites (KL1, KL2 and KL4). Each of these sites indicate clockwise rotations and their combined analysis indicates approximately 026 ± 10/43 ± 11° declination and inclination values, which indicate approximately 26° clockwise rotations for the Oligocene configuration of the domain. The second data set comprises six sites, and each of which indicates counter-clockwise rotations except the two Upper Miocene sites (TVS4 and TVS5) which indicate slight clockwise rotations. The combined analysis of the cluster indicate 345 ± 5°/43 ± 5 declination and inclination values which show approximately 15° counter-clockwise rotations of the Upper Miocene to Pliocene sequences of the domain.

Denizli Domain comprises six sites and only half of them produced interpretable results. Except one site with clockwise rotations (BD1), the other two sites produced counter-clockwise rotations. The combined analysis of all the sites indicate 344 ± 6°/59 ± 4° declination and inclination values, which indicate approximately 16° counter-clockwise rotation of the domain (Figs. 2b and 5).

Ulubey Domain is located at the north westernmost part of the study area (Fig. 2a). Out of 10 sites, two sites did not produce interpretable results; one site (UL2) produced results that indicate clockwise rotation while all other seven sites produced counter-clockwise rotations. Combined results of all the sites in the domain produced 355 ± 5°/49 ± 5° declination and inclination values, which indicates very subtle (∼5°) counter-clockwise rotation of the domain (Fig. 2b).

Dinar Domain contains only two sites (SK10 and BU4). Both sites produced counter-clockwise rotations. Combined analysis of these two sites produced 350 ± 9°/33 ± 14° declination and inclination values indicating approximately 10° counter-clockwise rotation of the domain. The tilt of the sampled horizons are almost horizontal so that in-situ and tectonic corrected values are almost the same.

Burdur Domain contains 10 sites, among these only 5 sites produced interpretable results (Table 1). The age of the sampled horizons are Pliocene (Özkaptan et al., 2018). Except the sites BU1 and RB1, which indicate slight counter-clockwise rotations. Combined analysis of all the sites in the domain indicate 357 ± 3°N/51 ± 3° declination and inclination values, which indicate approximately 3° counter-clockwise rotation of the domain.

Çameli Domain contains 12 sites and 8 them produced reliable results. The site M10 indicates remagnetization or present-day overprint, which could not be removed during the analysis. Sites M9 and PK6 did not produce any statistically meaningful results while the site M8 indicate present-day overprint, since declination and inclination values are close to present geomagnetic vector and after tectonic correction inclination become extremely shallower than expected position of the region during the Neogene. The ages of the sampled horizons are Upper Miocene to Pliocene (Alçiçek et al., 2017). Among these sites, except SK6, which produced normal polarity and the largest clockwise rotation value, the all other sites have reverse polarity and counter-clockwise rotations. Combined analysis of all the sites in the domain indicate 349 ± 6/50 ± 6 declination and inclination values, which indicate approximately 11° counter-clockwise rotation for the domain.

The Gölhisar Domain contains five sites and they are distributed uniformly in the domain (Fig. 2). All of the sites in the domain produced reliable results. All of them have reverse polarities and large counter-clockwise rotations, except the sites PK2 and site EL3 that have normal polarity and site EL3 indicates 10° clockwise rotation. Combined analysis of all the sites produced 339 ± 5°N/44 ± 6° declination and inclination values, which indicate approximately 21° counter-clockwise rotation for the domain.

Fethiye Domain contains two sets of data, the middle Miocene sites and Pliocene sites (Table 1). Except site FE1, other middle Miocene sites produced both normal and reverse polarities and both clockwise and counter-clockwise rotations. Combined analysis of these two middle Miocene sites indicate 354 ± 8°N/35 ± 11° declination and inclinations, which indicate approximately 6° counter-clockwise rotation of middle Miocene sequences in the domain. Two of the four sites sampled from the Pliocene sequences in the domain indicate normal polarity with clockwise rotation while the remaining two other sites indicate reverse polarity and counter-clockwise rotations. Combined analysis of the overall Pliocene sites produced 349 ± 7N/41° declination and inclination. This indicates that the domain has been rotated approximately 11° since Pliocene.

Elmalı Domain is the southeastern most domain of the study area (Fig. 2). The sampled horizons in the domain include Lower Miocene turbiditic fine clastics, marls and limestones. According to Morris and Robertson (1993) these Lower to Middle Miocene units were remagnetized by the end of the middle Miocene. The site ST6 produced reverse polarity and relatively higher inclination value, which is close to present day values, all other sites indicate normal polarities. Except for the sites EL2 and ST4, which have almost no rotations, all other sites consistently indicate counter-clockwise rotations around 25° ± 5°. Combined analysis of all the sites indicate 341 ± 2°N/26 ± 4° declination and very shallow inclination. These values indicate that the Elmalı Domain is rotated approximately 19° counter-clockwise by the end of middle Miocene.

5. Previous paleomagnetic studies

A number of previous paleomagnetic studies have been conducted in the region. Most of these studies are based on magmatic rocks or they target pre-Neogene units. However, the most recent studies addressing the Neogene units in the region and are relevant to this paper include Tatar et al. (2002) Gürsoy et al. (2003), van Hinsbergen et al. (2007, 2010a, 2010b), Koç et al. (2016) and Uzel et al. (2017). These studies are largely complementary to this study spatially and temporally (Fig. 2, Table 2).

Gürsoy et al. (2003) studied 82 volcanic sites around the Afyon Region and they combined these sites into five domains. The analysis of these data indicates that the Afyon Region experienced clockwise rotation as high as 25° since the Late Miocene. We parametrically resampled their results and reanalyzed using *paleomagnetism.org* for the sake of uniform processing routine with our data. According to this analysis, the Afyon Region experienced approximately 21° clockwise rotation since the late Miocene.

Tatar et al. (2002) studied Plio-Quaternary (4.7–2.5 Ma) volcanic rocks around the Isparta region and concluded that these volcanic rocks are rotated slightly clockwise with mean declination and inclination amounts of 006°N/53°. We parametrically resampled and analyzed their results, obtained 3.6 ± 3.8°N/58.5 ± 2.6° mean declination, and inclination values.

The areas in the northern part the study area that include mainly Uşak, Güre, Selendi and Demirci basins were studied by van Hinsbergen et al. (2010a). They grouped these basins as North Menderes Basins (Fig. 2b). All of these basins indicate clockwise rotation and their combined analysis yielded approximately 14° ± 9° clockwise rotations. We parametrically resampled their data and obtained almost exactly same results (Table 1).

Similarly, the parametrically resampled data of van Hinsbergen et al. (2010b) from Gölhisar-Çameli, and Burdur domains produced almost the same results with our findings. The results from the Kale Domain, which overlaps with our Kale-Tavas Miocene sites, indicate approximately 20° ± 3° counter-clockwise rotations which we found 14° ± 5° from the same area. The Acıpayam domain of van Hinsbergen et al. (2010c) comprises lower Miocene sequences and yielded approximately 9° ± 3° and it partly overlaps spatially with our Çameli Domain, which we found approximately 11° ± 6° counter-clockwise rotations. In addition, the Kelekçi Domain of van Hinsbergen et al. (2010a) is located within our Çameli Domain and yielded 13° ± 7 counter-clockwise rotation similar to our results.

The Korkuteli and Doğantaş sections of van Hinsbergen et al. (2010b) comprise lower-middle Miocene units. This area spatially complements our study area. All of these sections indicate more than 20° counter-clockwise rotation of the Beydağları Platform by middle Miocene. According to Morris and Robertson (1993), the Beydağları platform experienced a widespread middle Miocene remagnetization event. However, van Hinsbergen et al. (2010b) argued that middle Miocene remagnetization is not as widespread as proposed. They reported both normal and reverse polarities that correlate with geomagnetic polarity timescale, existing in the lower Miocene turbiditic sequences of Korkuteli and Doğantaş sections with positive fold test. This implies that the remagnetism in the region is local and the Beydağları Platform rotated around 20° from middle Miocene.

The easternmost part of the studied region comprises Aksu Domain. Although the northern and southern parts of the basin have slight variations in the rotation amounts, however, overall rotation in the basin is negligible (Koç et al., 2016). Here we parametrically resampled all the reliable data from the northern and southern parts of the basin and obtained 359 ± 6.2 declination and 46 ± 2.6° inclination values, which indicates almost no rotation of the Aksu Domain.

Söke Domain is located at the westernmost part of the study area. Uzel et al. (2017) reported that the basin underwent approximately 28 ± 2.6° counter-clockwise rotation during the lower Miocene and 23 ± 5° clockwise rotation during the upper Miocene. The basin is located within the İzmir–Balıkesir Transfer Zone and its rotation is related to the activity of the transfer zone (Uzel et al., 2015).

The island of Rhodes comprises uplifted Pliocene marine sequences. These units experienced two phases of counter-clockwise rotations, which collectively indicate 26° ± 5° rotation (van Hinsbergen et al., 2007).

6. Discussions

6.1. Interpretation of results

The literature data and our results indicate that there are three main rotation domains in the study area. These include SW Anatolian Domain (SWAD), Burdur–Dinar–Ulubey Domain, and the areas north of these domains. The boundaries of these domains are well defined by regional structures, such as Büyük Menderes Graben, Acıpayam Transfer Zone, Dinar and Aksu faults (Figs. 2 and 6).

The northern areas are clearly separated from the Burdur–Dinar–Ulubey and the SW Anatolian domains by major regional faults. We have not studied in this region but the parametrically resampled and reanalysed literature data (Gürsoy et al., 2003; van Hinsbergen et al. (2010b); Uzel et al., 2017) obtained mainly from volcanic rocks and some sedimentary sequences in this domain indicate clockwise rotations with gradual increase from 5.5 ± 9.6°

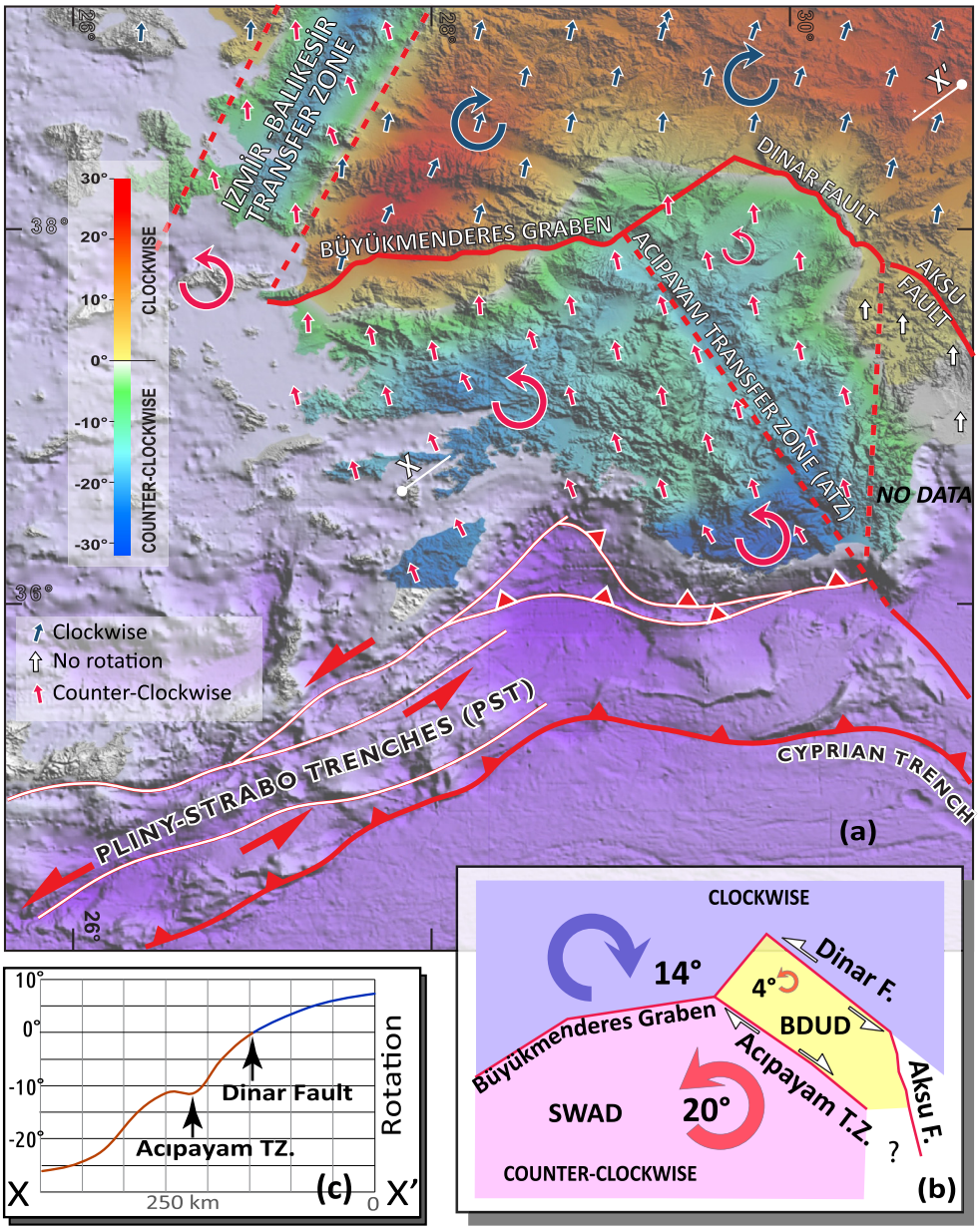

Fig. 6. (a) Image of interpolated declinations with declination arrows depicting the regions with clockwise, counter-clockwise and no rotations. (b) Cross-section along the line XX' depicting how the rotation amounts change in NE-SW directions. (c) Simplified map illustrating the rotational domains and mean rotation amounts.

around Ayvalık-Bergama area in the west to 20 ± 6° except for the upper Miocene rotations of Söke Domain (Uzel et al., 2017) and within the İzmir–Balıkesir Transfer Zone. In the analyses# the İBTZ is not elaborated here for the sake of simplicity and the rotations within the zone are related directly to fault movements (Uzel et al., 2013, 2015).

The Burdur–Dinar–Ulubey Domain (BDUD) includes the Ulubey, Dinar, and Burdur domains and Aksu Domain of Koç et al. (2016). The rotation amounts in this domain are slightly counter-clockwise (∼4°) despite some sites in the domain have both clockwise and counter-clockwise rotations as high as 10° (Fig. 2). The northwestern boundary of BDUD is defined by the boundary faults of the Uşak Basin while the northern and the eastern boundaries are defined by the Dinar and Aksu faults respectively. Further in the southeast, its boundary is not well defined due to lack of Neogene deposits in this region for paleomagnetic sampling.

The SW Anatolian Domain comprises all the sites and the areas south of Burdur–Dinar–Ulubey Domain. Within the domain only the Oligocene sequences of the Tavas Domain are rotated clockwise coherently, while all other Miocene and Pliocene sites that include the Acıpayam, Gölhisar, Fethiye, Kelekçi, Denizli, Miocene sequences of the Tavas, Ören and Didim domains as well as and Kale domains of van Hinsbergen et al. (2010a, 2010b) indicate counter-clockwise rotations. The rotation amounts might vary on the site basis; however the mean rotation of the domain is around 20° counter-clockwise. In addition, areas located on the Beydağları Platform that include the Elmalı Domain and the Korkuteli and Doğantaş sequences of van Hinsbergen et al. (2010b) all collectively indicate approximately ∼20 counter-clockwise rotation by the middle Miocene onwards (Fig. 6b).

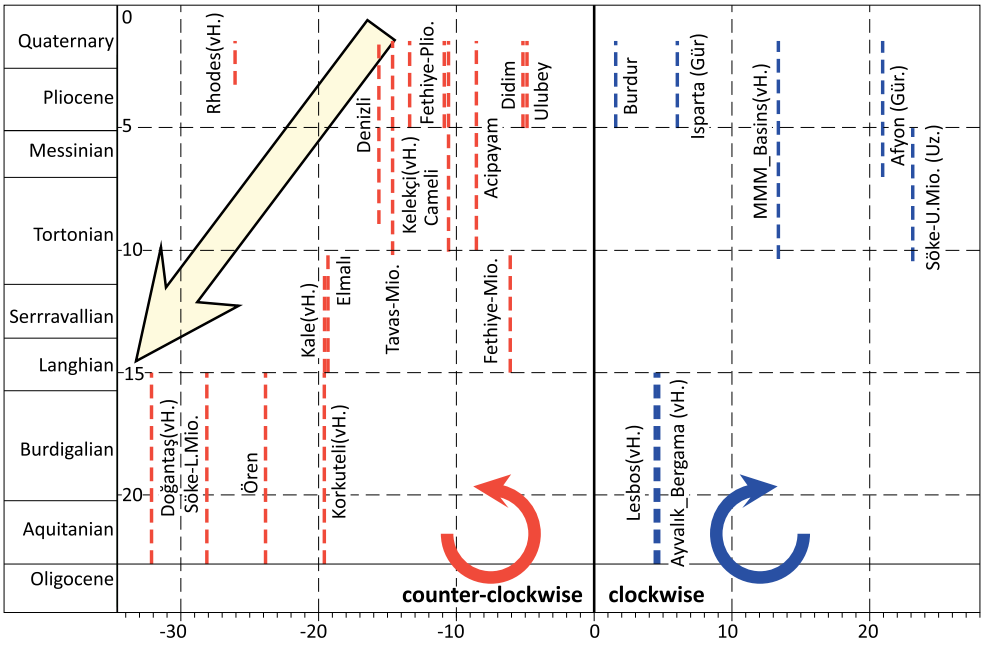

Fig. 7. Temporal relationship of rotations obtained in this study and from the literature. Note a subtle increase in the counter-clockwise rotations in time. vH.: van Hinsbergen et al. (2007, 2010a, 2010b), Gür: Gürsoy et al. (2003), Uz: Uzel et al. (2017).

6.2. Spatio-temporal relationships

Most of the paleomagnetic data studied and analysed in this study were collected mainly from Miocene to Pliocene units (Table 1) except for the Tavas Domain. The oldest Neogene samples were collected from the lower Miocene sequences of the Ören and Fethiye basins. Although, the samples from the Elmalı Domain were collected from the lower Miocene units, they were re-magnetized during the middle Miocene (Morris and Robertson, 1993) therefore, the information obtained from this domain represents the post-middle Miocene rotations. In order to assess the temporal relationship between rotations and age of the sampled rocks, the rotations from all sites were plotted against the age of the rocks (Fig. 7). Although, the largest rotation amounts are associated with the oldest units from the Ören and Elmalı domains, the ages of the rotations were not constrained to any time interval since the rotations took place at every stage of the Neogene. This relationship implies that the rotations in the region are not episodic but took place possibly continuously through the Neogene period indicating continuous deformation in the region.

In order to evaluate the spatial variation of the rotation amounts, the mean rotation values at the domain centres were interpolated throughout the study area. During the interpolation procedure the interpolation was tweaked at the boundaries of the domains by adding extra sites just for obtaining sharp transitions at the domain boundaries that matches with the domain bounding faults (Fig. 6a). As shown in the figure obviously there is almost linear increase in the rotation amounts along N-S direction while there is no major change in the rotation amounts along E-W direction. On the cross-section along the line XX', the location of the Acıpayam Accommodation Zone is marked with sharp change in the rotation amounts (Fig. 6c).

6.3. Regional implications

A tear in the subducted lithosphere of the African slab along the Pliny-Strabo Trench was already recognized previously Wortel and Spakman, 2000; Faccenna et al., 2006; van Hinsbergen et al., 2010c; Biryol et al., 2011; Özbakir et al., 2013. The main debate about this structure is related to its continuation into the overriding plate. According to Hall et al. (2014) this STEP fault continues north-eastwards into SW Anatolia, far beyond the present positions of the Pliny-Strabo and Cyprian trenches as wide as 80 km as a sinistral strike-slip shear zone. Strike-slip faults and STEP faults have common characteristics such as differential rotations at different parts of the fault zone and on either sides of the fault zone as well. Govers and Wortel (2005) suggested that the amount of rotation increases from the point of tear towards the trench along a STEP fault due to differential retreating of the trench on either side of the STEP fault. Increase in the rotation amounts towards the trench on the over-riding plate is a common phenomenon in retreating curved trenches or orogenic belts (e.g. Martin, 2013). However, sharp contrasts in the rotations along a zone require development of tectonic discontinuity, such as a strike-slip or a STEP fault.

The rotational deformation of the Greece and the Aegean region is well established in the literature (Duermeijer et al., 2000; van Hinsbergen et al., 2005). According to van Hinsbergen et al. (2005), the mainland Greece underwent more than 50° clockwise rotation by the middle Miocene. In the meantime, the SE Aegean islands experienced counter-clockwise rotations (Duermeijer et al., 2000; van Hinsbergen et al., 2007). However, the rotations in the eastern part of the Aegean and western Turkey is much more complex. This is due to involvement of a number of strike-slip faults associated with the North Anatolian Fault Zone and the İzmir–Balıkesir Transfer Zone (Kaymakci et al., 2007; Kissel et al., 2003; Piper et al., 2010; Uzel et al., 2013, 2015) in the region. Apart from these fault zones, Western Anatolian region is dominated by clockwise rotations approximately north of the 38° latitude, while south of it is dominated by counter-clockwise rotations. The counter-clockwise rotations increase southwards and westwards from around Aksu and Burdur domains where there are negligible rotations (Fig. 6). We suggest that such deformation styles and rotations can be conceptualized as a differentially stretching rubber sheet (Fig. 8a) where the locus of the largest extension is located at the SW margin of the study area. The main driving force behind the rotations in the region is the retreat of the African Slab west of the Pliny Strabo STEP fault (Fig. 8b). As the trench mi-

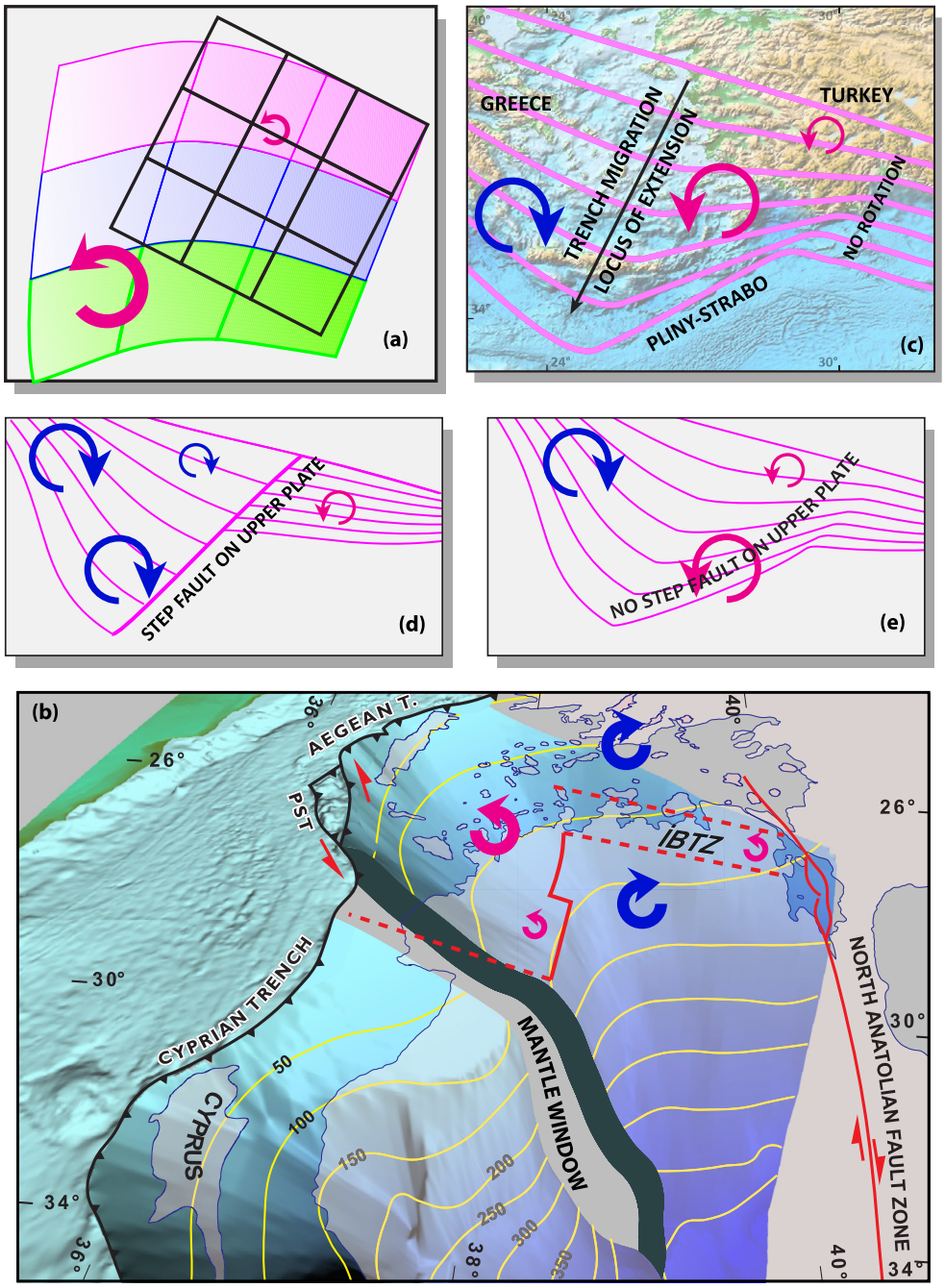

Fig. 8. (a) Stretched rubber sheet analogy to explain the rotations in the study area. (b) 3D geometry of the subducted north African Oceanic lithosphere (after Biryol et al., 2011) manifesting the location of torn-apart slab, mantle window and rotating blocks on the over-riding plate. Contours are depths in kilometre. (c) Palinspastic reconstruction of trench positions in the Aegean region since early Miocene. (d) Trench position scenario, in the case of STEP Fault propagates into the over-riding plate, and (e) Trench position scenario in the case of STEP fault does not propagate into the over-riding plate, down-going plates are not coupled. Note rotations in various scenarios. IBTZ: İzmir–Balıkesir Transfer Zone, PST: Pliny-Strabo Trench.

grated southwards it gave way to the clockwise rotation of Greece and counter-clockwise rotations of the SW Anatolia (Fig. 8c). In this context, the main question is related to if the tear in the subducted African slab is propagated into the over-riding plate.

Hall et al. (2014), Elitez et al. (2016), Elitez and Yaltırak (2016) claimed that the Pliny-Strabo STEP Fault is propagated northwestwards into SW Anatolia as a sinistral strike-slip fault zone. They claimed that it is a transtensional sinistral strike-slip fault zone as wide as 80 km and named it as Fethiye–Burdur Shear Zone. However, they failed to provide any tangible data that proves presence of any major strike-slip fault in the region. Alçiçek (2015) and Özkaptan et al. (2018) argued that there is no kinematic evidence from the alleged shear zone that substantiate presence of any NE-SW striking strike-slip fault in the region based. They based their arguments on the extensive paleostress inversion studies carried out in the region. Interestingly, most of the kinematic and moment tensor solutions provided by the works both opposing and in favour of the existence of Fethiye Burdur Shear Zone indicate normal faults with some oblique components.

Like most major strike-slip faults, it is expected that the rotation amounts and/or senses need to be changed sharply within and/on either side of such a structure. As in the case of the İzmir–Balıkesir Fault Zone (Uzel et al., 2015) and the North Anatolian Fault Zone (Kaymakci et al., 2007) regardless of the origin of the

structure. It might be STEP fault, a transcurrent fault related collision or transfer fault in an extensional setting. The results of this study indicate that there is no differential rotation along the position and wholesale extent of the alleged Fethiye–Burdur Shear Zone as proposed previously.

We claim that the rotations in the study area were resulted from tearing and differential retreat of Aegean and Cyprian trenches, both of which have been retreating but Aegean trench was faster similar to present-day velocities obtained from GPS vectors (Reilinger et al., 2006). We suggest that as the trench retreated southwards from about 38°N latitudinal positions in the study area during the lower Miocene (Jolivet and Brun, 2010) to present position gradually. This resulted in gradual change in the intensity in the deformation and rotation amounts along E-W directions. In Fig. 8d–e, two scenarios are illustrated. In case of STEP fault propagated into the over-riding plate, Fethiye–Burdur Shear Zone case, the region would be dominated by clockwise rotations. In the second case, STEP fault is not propagated into the over-riding plate and clockwise rotations are developed in the west while counter-clockwise rotations are developed in a very wide region. In addition, there is no differential rotation on either side of the alleged shear zone. However, the main differential rotations took place along the Dinar and Aksu faults, and the Acıpayam Transfer Zone. Due to lack of differential rotations along the proposed Fethiye–Burdur Fault Zone and lack of any kinematic data supporting presence of any NE-SW striking major sinistral strike-slip fault zone in the region (Alçiçek, 2015; Özkaptan et al., 2018) implies that existence of Fethiye–Burdur Fault (or Shear) is dubious.

7. Conclusions

A through and comprehensive paleomagnetic sampling and analysis has been carried out to unravel the interplay between STEP fault development in the subducted northern edge of the African oceanic lithosphere and the over-riding plate in the SW Anatolia. The results have shown that there are three main rotation domains in the area. These are, from south to north, include (1) SW Anatolian domain characterized by counter-clockwise rotations, which increases southwards, (2) the Burdur–Ulubey–Dinar Domain, which is characterized by minimal counter-clockwise rotation.

The most important conclusion of these results is that the Pliny-Strabo STEP fault is not coupled with and did not propagate into the over-riding plate in the SW Anatolia. This is evidenced by the lack of differential rotations in NE directions along its possible northern extension along the alleged Fethiye Burdur Fault (or Shear) Zone. Therefore, there is no paleomagnetic evidence to support the existence of the Fethiye Burdur Fault/Shear Zone.

Acknowledgements

This study is supported by Scientific and Technological Research Council of Turkey, Grant number TÜBİTAK – 111Y239. We would like to thank Pinar Ertepinar and Ayten Koç for field assistance.

Appendix A. Supplementary material

Supplementary material related to this article can be found online at https://doi.org/10.1016/j.epsl.2018.06.022.

References

Alçiçek, H., Wesselingh, F.P., Alçiçek, M.C., Jiménez-Moreno, G., Feijen, F.J., van den Hoek Ostende, L.W., Mayda, S., Tesakov, A.S., 2017. A multiproxy study of the early Pleistocene palaeoenvironmental and palaeoclimatic conditions of an anastomosed fluvial sequence from the Çameli Basin (SW Anatolia, Turkey). Palaeogeogr. Palaeoclimatol. Palaeoecol. 467, 232–252. https://doi.org/10.1016/j.palaeo.2016.08.019.

Alçiçek, M.C., 2007. Tectonic development of an orogen-top rift recorded by its terrestrial sedimentation pattern: the Neogene Eşen Basin of southwestern Anatolia, Turkey. Sediment. Geol. 200, 117–140. https://doi.org/10.1016/j.sedgeo.2007.04.003.

Alçiçek, M.C., 2015. Comment on "The Fethiye–Burdur Fault Zone: a component of upper plate extension of the subduction transform edge propagator fault linking Hellenic and Cyprus Arcs, Eastern Mediterranean. Tectonophysics 635, 80–99" by J. Hall, A.E. Aksu, İ. Elitez, C. Yaltırak, G. Çiftçi. Tectonophysics 664, 1–4. https://doi.org/10.1016/j.tecto.2015.01.025.

Alçiçek, M.C., Brogi, A., Capezzuoli, E., Liotta, D., Meccheri, M., 2013. Superimposed basin formation during Neogene–Quaternary extensional tectonics in SW-Anatolia (Turkey): insights from the kinematics of the Dinar Fault Zone. Tectonophysics 608, 713–727. https://doi.org/10.1016/j.tecto.2013.08.008.

Alçiçek, M.C., Kazanci, N., Özkul, M., 2005. Multiple rifting pulses and sedimentation pattern in the Çameli Basin, southwestern Anatolia, Turkey. Sediment. Geol. 173, 409–431. https://doi.org/10.1016/j.sedgeo.2003.12.012.

Barka, A., Reilinger, R., 1997. Active tectonics of the Eastern Mediterranean region: deduced from GPS, neotectonic and seismicity data. Ann. Geophys. 40 (3).

Biryol, C., Beck, S.L., Zandt, G., Özacar, A.A., 2011. Segmented African lithosphere beneath the Anatolian region inferred from teleseismic P-wave tomography. Geophys. J. Int. 184, 1037–1057. https://doi.org/10.1111/j.1365-246X.2010.04910.x.

Butler, R.F., 1992. Paleomagnetism: Magnetic Domains to Geologic Terranes, vol. 319. Blackwell Scientific Publications, Boston.

Chulliat, A., Maus, S., 2014. Geomagnetic secular acceleration, jerks, and a localized standing wave at the core surface from 2000 to 2010. J. Geophys. Res., Solid Earth 119 (3), 1531–1543.

Deenen, M.H., Langereis, C.G., van Hinsbergen, D.J., Biggin, A.J., 2011. Geomagnetic secular variation and the statistics of palaeomagnetic directions. Geophys. J. Int. 186 (2), 509–520.

Duermeijer, C.E., Nyst, M., Meijer, P.T., Langereis, C.G., Spakman, W., 2000. Neogene evolution of the Aegean arc: paleomagnetic and geodetic evidence for a rapid and young rotation phase. Earth Planet. Sci. Lett. 176, 509–525.

Dumont, J.F., Poisson, A., Sahinci, A., 1979. Sur l'existence de coulissements sinistres recentes a l'extermité orientale de l'arc ageen (sud-ouest de la Turquie). C. R. Acad. Sci. Paris 289, 261–264.

Elitez, İ., Yaltırak, C., 2016. Miocene to Quaternary tectonostratigraphic evolution of the middle section of the Burdur–Fethiye Shear Zone, south-western Turkey: implications for the wide inter-plate shear zones. Tectonophysics 690, 336–354. https://doi.org/10.1016/j.tecto.2016.10.003.

Elitez, İ., Yaltırak, C., Aktuğ, B., 2016. Extensional and compressional regime driven left-lateral shear in southwestern Anatolia (eastern Mediterranean): the Burdur–Fethiye Shear Zone. Tectonophysics 688, 26–35. https://doi.org/10.1016/j.tecto.2016.09.024.

Faccenna, C., Bellier, O., Martinod, J., Piromallo, C., Regard, V., 2006. Slab detachment beneath eastern Anatolia: a possible cause for the formation of the North Anatolian Fault. Earth Planet. Sci. Lett. 242, 85–97.

Fisher, R., 1953. Dispersion on a sphere. Proc. R. Soc. Lond. Ser. A, Math. Phys. Sci. 217 (1130), 295–305.

Gong, Z., Langereis, C.G., Mullender, T.A.T., 2008. The rotation of Iberia during the Aptian and the opening of the Bay of Biscay. Earth Planet. Sci. Lett. 273 (1–2), 80–93.

Govers, R., Wortel, M.J.R., 2005. Lithosphere tearing at STEP faults: response to edges of subduction zones. Earth Planet. Sci. Lett. 236, 505–523.

Gürsoy, H., Piper, J.D.A., Tatar, O., 2003. Neotectonic deformation in the western sector of tectonic escape in Anatolia: palaeomagnetic study of the Afyon region, central Turkey. Tectonophysics 374, 57–79. https://doi.org/10.1016/S0040-1951(03)00346-9.

Hall, J., Aksu, A.E., Elitez, I., Yaltirak, C., Çifçi, G., 2014. The Fethiye–Burdur Fault Zone: a component of upper plate extension of the subduction transform edge propagator fault linking Hellenic and Cyprus Arcs, Eastern Mediterranean. Tectonophysics 635, 80–99. https://doi.org/10.1016/j.tecto.2014.05.002.

Hayward, A.B., 1984. Miocene clastic sedimentation related to the emplacement of the Lycian Nappes and the Antalya Complex, S.W. Turkey. In: Dixon, J.E., Robertson, A.H.F. (Eds.), Geological Evolution of the Eastern Mediterranean. In: Geological Society of London Special Publication, pp. 287–300.

Huang, W., Dupont-Nivet, G., Lippert, P.C., Van Hinsbergen, D.J., Hallot, E., 2013. Inclination shallowing in Eocene Linzizong sedimentary rocks from Southern Tibet: correction, possible causes and implications for reconstructing the India–Asia collision. Geophys. J. Int. 194 (3), 1390–1411.

Jolivet, L., Brun, J.P., 2010. Cenozoic geodynamic evolution of the Aegean. Int. J. Earth Sci. 99, 109–138. https://doi.org/10.1007/s00531-008-0366-4.

Kaymakci, N., 2006. Kinematic development and paleostress analysis of the Denizli Basin (Western Turkey): implications of spatial variation of relative paleostress magnitudes and orientations. J. Asian Earth Sci. 27. https://doi.org/10.1016/j.jseaes.2005.03.003.

Kaymakci, N., Aldanmaz, E., Langereis, C.G., Spell, T.L., Gurer, O.F., Zanetti, K.A., 2007. Late Miocene transcurrent tectonics in NW Turkey: evidence from palaeomagnetism and 40Ar–39Ar dating of alkaline volcanic rocks. Geol. Mag. 144, 379–392.

Kaymakci, N., Inceöz, M., Ertepinar, P., Koç, A., 2010. Late Cretaceous to Recent kinematics of SE Anatolia (Turkey). In: Geological Society Special Publications.

Kaymakci, N., Langereis, C., Özkaptan, M., Özacar, A.A., Gülyüz, E., Uzel, B., Sözbilir, H., 2017. Fethiye–Burdur Fault Zone (SW Turkey): a myth? In: General Assembly Conference Abstracts, vol. 19, p. 5443.

Kirschvink, J.L., 1980. The least-squares line and plane and the analysis of palaeomagnetic data. Geophys. J. Int. 62 (3), 699–718.

Kissel, C., Laj, C., Poisson, A., Görür, N., 2003. Paleomagnetic reconstruction of the Cenozoic evolution of the Eastern Mediterranean. Tectonophysics 362, 199–217.

Koç, A., van Hinsbergen, D.J., Kaymakci, N., Langereis, C.G., 2016. Late Neogene oroclinal bending in the central Taurides: a record of terminal eastward subduction in southern Turkey? Earth Planet. Sci. Lett. 434, 75–90.

Konak, N., Şenel, M., 2002. Türkiye'nin 1/500.000 ölçekli jeoloji haritası. Denizli bölgesi. MTA, Ankara.

Koymans, M.R., Langereis, C.G., Pastor-Galán, D., van Hinsbergen, D.J., 2016. Paleomagnetism.org: an online multi-platform open source environment for paleomagnetic data analysis.

Martin, A.K., 2013. Double-saloon-door tectonics in the North Fiji Basin. Earth Planet. Sci. Lett. 374, 191–203. https://doi.org/10.1016/j.epsl.2013.05.041.

McFadden, P.L., McElhinny, M.W., 1988. The combined analysis of remagnetization circles and direct observations in palaeomagnetism. Earth Planet. Sci. Lett. 87 (1–2), 161–172.

Morris, A., Robertson, A.H.F., 1993. Miocene remagnetisation of carbonate platform and Antalya Complex units within the Isparta Angle, SW Turkey. Tectonophysics 220, 243–266.

Mullender, T.A., Frederichs, T., Hilgenfeldt, C., de Groot, L.V., Fabian, K., Dekkers, M.J., 2016. Automated paleomagnetic and rock magnetic data acquisition with an in-line horizontal "2G" system. Geochem. Geophys. Geosyst. 17 (9), 3546–3559.

Mullender, T.A.T., Velzen, A., Dekkers, M.J., 1993. Continuous drift correction and separate identification of ferrimagnetic and paramagnetic contributions in thermomagnetic runs. Geophys. J. Int. 114 (3), 663–672.

Özbakir, A.D., Şengör, A.M.C., Wortel, M.J.R., Govers, R., 2013. The Pliny-Strabo trench region: a large shear zone resulting from slab tearing. Earth Planet. Sci. Lett. 375, 188–195. https://doi.org/10.1016/j.epsl.2013.05.025.

Özkaptan, M., Kaymakci, N., Langereis, C.G., Gülyüz, E., Özacar, A.A., Uzel, B., Sözbilir, H., 2018. Age and kinematics of the Burdur Basin: inferences for the Fethiye Burdur Fault Zone in SW Anatolia (Turkey). Tectonophysics. In press.

Philippon, M., Willingshofer, E., Sokoutis, D., Corti, G., Sani, F., Bonini, M., Cloetingh, S., 2015. Slip re-orientation in oblique rifts. Geology 43, 147–150. https://doi.org/10.1130/G36208.1.

Piper, J.D.A., Gürsoy, H., Tatar, O., Beck, M.E., Rao, A., Koçbulut, F., Mesci, B.L., 2010. Distributed neotectonic deformation in the Anatolides of Turkey: a palaeomagnetic analysis. Tectonophysics 488, 31–50. https://doi.org/10.1016/j.tecto.2009.05.026.

Reilinger, R., McClusky, S., Vernant, P., Lawrence, S., Ergintav, S., Cakmak, R., Ozener, H., Kadirov, F., Guliev, I., Stepanyan, R., Nadariya, M., Hahubia, G., Mahmoud, S., Sakr, K., ArRajehi, A., Paradissis, D., Al-Aydrus, A., Prilepin, M., Guseva, T., Evren, E., Dmitrotsa, A., Filikov, S.V., Gomez, F., Al-Ghazzi, R., Karam, G., 2006. GPS constraints on continental deformation in the Africa–Arabia–Eurasia continental collision zone and implications for the dynamics of plate interactions. J. Geophys. Res., Solid Earth 111. https://doi.org/10.1029/2005JB004051.

Salaün, G., Pedersen, H.A., Paul, A., Farra, V., Karabulut, H., Hatzfeld, D., Papazachos, C., Childs, D.M., Pequegnat, C., 2012. High-resolution surface wave tomography beneath the Aegean–Anatolia region: constraints on upper-mantle structure. Geophys. J. Int. 190, 406–420. https://doi.org/10.1111/j.1365-246X.2012.05483.x.

Sözbilir, H., 2005. Oligo–Miocene extension in the Lycian orogen: evidence from the Lycian molasse basin, SW Turkey. Geodin. Acta 18, 255–282. https://doi.org/10.3166/ga.18.255-282.

Tatar, O., Gursoy, H., Piper, J.D.A., 2002. Differential neotectonic rotations in Anatolia and the Tauride Arc: palaeomagnetic investigation of the Erenlerda Volcanic Complex and Isparta volcanic district, south-central Turkey. J. Geol. Soc. (Lond.) 159, 281–294. https://doi.org/10.1144/0016-764901-035.

Uzel, B., Langereis, C.G., Kaymakci, N., Sözbilir, H., Özkaymak, Ç., Özkaptan, M., 2015. Paleomagnetic evidence for an inverse rotation history of Western Anatolia during the exhumation of Menderes core complex. Earth Planet. Sci. Lett. 414, 108–125.

Uzel, B., Sözbilir, H., Özkaymak, Çağlar, Kaymakci, N., Langereis, C.G., 2013. Structural evidence for strike-slip deformation in the Izmir–Balikesir transfer zone and consequences for late Cenozoic evolution of western Anatolia (Turkey). J. Geodyn. 65, 94–116. https://doi.org/10.1016/j.jog.2012.06.009.

Uzel, B., Sümer, Ö., Özkaptan, M., Özkaymak, Ç., Kuiper, K., Sözbilir, H., Kaymakci, N., İnci, U., Langereis, C.G., 2017. Palaeomagnetic and geochronological evidence for a major middle miocene unconformity in Söke Basin (western Anatolia) and its tectonic implications for the Aegean region. J. Geol. Soc. (Lond.) 174. https://doi.org/10.1144/jgs2016-006.

van Hinsbergen, D.J.J., Dekkers, M.J., Bozkurt, E., Koopman, M., 2010a. Exhumation with a twist: paleomagnetic constraints on the evolution of the Menderes metamorphic core complex, western Turkey. Tectonics 29, 1–33. https://doi.org/10.1029/2009TC002596.

van Hinsbergen, D.J.J., Dekkers, M.J., Koç, A., 2010b. Testing Miocene remagnetization of Bey Dağları: timing and amount of Neogene rotations in SW Turkey. Turk. J. Earth Sci. 19, 123–156. https://doi.org/10.3906/yer-0904-1.

van Hinsbergen, D.J.J., Kaymakci, N., Spakman, W., Torsvik, T.H., 2010c. Reconciling the geological history of western Turkey with plate circuits and mantle tomography. Earth Planet. Sci. Lett. 297, 674–686.

van Hinsbergen, D.J.J., Krijgsman, W., Langereis, C.G., Cornee, J.-J., Duermeijer, C.E., van Vugt, N., 2007. Discrete Plio-Pleistocene phases of tilting and counterclockwise rotation in the southeastern Aegean arc (Rhodos, Greece): early Pliocene formation of the south Aegean left-lateral strike-slip system. J. Geol. Soc. (Lond.) 164, 1133–1144. https://doi.org/10.1144/0016-76492006-061.

van Hinsbergen, D.J.J., Langereis, C.G., Meulenkamp, J.E., 2005. Revision of the timing, magnitude and distribution of Neogene rotations in the western Aegean region. Tectonophysics 396, 1–34. https://doi.org/10.1016/j.tecto.2004.10.001.

Wortel, M.J.R., Spakman, W., 2000. Subduction and Slab Detachment in the Mediterranean–Carpathian region. Science 80 (290), 1910–1917. https://doi.org/10.1126/science.290.5498.1910.